ORIGINAL ARTICLE

A C G publications

Rec. Nat. Prod. X:X (202X) XX-XX

records of natural products

Isolation of New Secondary Metabolites from *Kedrostis gijef* and Evaluation of Their *α*-Glucosidase Inhibitory Activity

Mahmoud M. Mubarek [1,2], Fahd M. Abdelkarem [1,3], Ahmed Othman [4], Masako Matsumoto [1], Fangjing Li [1] and Kuniyoshi Shimizu [1*]

[1] *Department of Agro-Environmental Sciences, Graduate School of Bioresource and Bioenvironmental Sciences, Kyushu University, Fukuoka, 819-0395, Japan*

[2] *Department of Medicinal and Aromatic plants, Desert Research Center, Matariya, Cairo, 11753, Egypt*

[3] *Department of Pharmacognosy, Faculty of Pharmacy, Al-Azhar University, Assiut, 71524, Egypt.*

[4] *Department of Pharmacognosy and Medicinal Plants, Faculty of Pharmacy, Al-Azhar University, Cairo, 11884, Egypt*

(Received May 23, 2024; Revised June 26, 2024; Accepted June 27, 2024)

Abstract: Four new polyoxygenated cucurbitane triterpene glycosides named kedrojiftene A-D **(4-7),** were isolated *via* different chromatographic techniques along with three phenolic compounds (**1-3**) from the crude extract of *Kedrostis gijef*. The isolated compounds were elucidated based on 1D, 2D-NMR spectroscopic analyses, HRESIMS and comparison with the related metabolites in literature. In bioassay, the *α*-glucosidase inhibitory assay for the isolated compounds was carried out and compounds **(1-3)** showed significant inhibitory activities.

Keywords: *Kedrostis gijef;* triterpene; cucurbitane; phenolic; *α*-glucosidase.

1. Introduction

The Cucurbitaceae family comprises approximately 965 species and about 95 genera [1, 2]. Plants belonging to the Cucurbitaceae family are recognized as reservoirs of bioactive metabolites with significant therapeutic potential. The metabolites extracted from these plants, such as, alkaloids, polyphenols, saponins, carotenoids, phytosterols, and cucurbitane type triterpenoids, have exhibited diverse bioactivities such as anti-inflammatory, immunomodulatory, hepatoprotective, antioxidant, antidiabetic, and cytotoxic properties [3-5].

Kedrostis genus encompasses around 35 species of climbing or trailing herbs. Studies have shown that the crude extract of *Kedrostis foetidissima* leaves possesses antioxidant properties. Additionally, the leaves of the phenolic-rich fraction of *K. foetidissima* demonstrated a protective effect against cardiac toxicity in rats by restoring cardiac antioxidant function[6]. Furthermore, *K. Africana* showed antimicrobial and antioxidant properties [7].

* Corresponding author: E-Mail: shimizu@agr.kyushu-u.ac.jp

The article was published by ACG Publications
http://www.acgpubs.org/journal/records-of-natural-products Month-Month 202x EISSN:1307-6167
DOI: http://doi.org/10.25135/rnp.468.2405.3236
Available online: July 20, 2024

Isolation of new secondary metabolites

Kedrostis gijef (Forssk. ex J.F.Gmel.) C. Jeffrey., is a climber plant, distributed in Gebel Elba (Egypt), Sudan, Ethiopia, Kenya, Tanzania, Somalia and Saudi Arabia [8]. However, rare phytochemical studies were carried out on this plant, and indicated presence of flavonoids, saponins, and tannins [9] .This encouraged us to make a detailed phytochemical investigations and evaluation of the *in vitro α-* glucosidase inhibitory activity for the isolated compounds. The phytochemical investigation of *K. gijef* aerial parts resulted in the isolation of seven compounds including four new cucurbitane type triterpene glycosides (**4-7**) and three phenolic compounds (**1-3**) and evaluation of *α*-glucosidase inhibitory assay of the isolated compound.

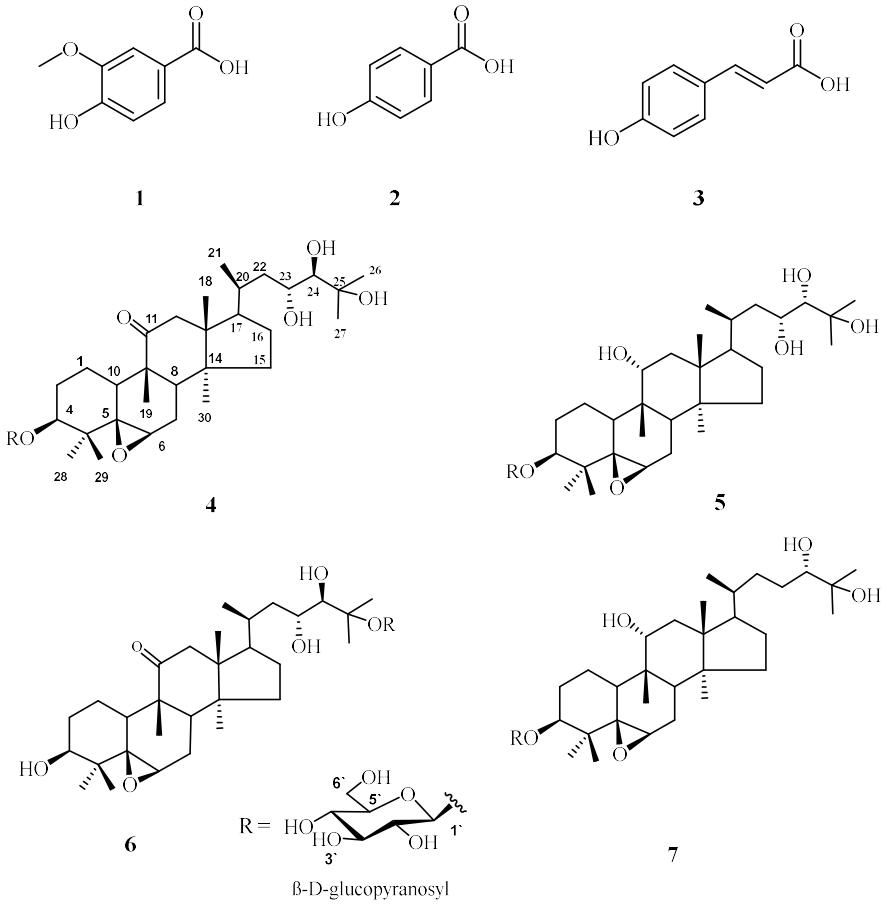

Figure 1. Structure of compounds **1-7** isolated from *Kedrostis gijef*

2. Materials and Methods

2.1. General Procedures

Optical rotations were measured using a Jasco P-2200 polarimeter (Jasco, Tokyo, Japan). The NMR spectra of the isolated compounds were acquired using a Bruker DRX-600 spectrometer (Bruker Daltonics, Billerica MA, USA) with tetramethyl silane (TMS) as an internal standard. The chemical shifts were reported as *δ* values. The high-resolution mass spectrometry (HR-ESI-MS) data of the compounds were obtained using a quadrupole time-of-flight (qTOF) mass spectrometer (Agilent Technologies, USA). The organic solvents utilized for extraction and purification, *n*-hexane, dichloromethane (DCM), ethyl acetate (EtOAc), *n*-butanol (BuOH), formic acid (FA), methanol (MeOH), acetonitrile (ACN), were purchased from Wako Pure Chemical Industries, based in Osaka, Japan. For further fractionation, a Biotage Selekt system from Uppsala, Sweden, equipped with NP-silica gel was employed.

Isolation and purification of the compounds was accomplished using a MPLC Pure C-850 Flash Prep® system from Buchi, located in Flawil, Switzerland. This system features UV and

evaporative light scattering detector (ELSD) detection. A HPLC preparative column (Inertsil ODS-3, 5 µm, 20 × 250 mm) obtained from GL Sciences Inc., Japan.
TLC silica gel 60 F254 plates were obtained from Merck, a company based in Darmstadt, Germany and the methanol-d_4 (CD_3OD) was purchased from Cambridge Isotope Laboratories, situated in Andover, MA, USA.

2.2. Plant Material

The aerial parts of *K. gijef* were collected from Wadi Elshallal, Gebel Elba (22˚04'50.8"N 36˚31'09.2"E) during April 2019 and identified by Dr. Mahmoud Ali, Associate Professor of Plant Ecology, and Dr. rer. nat. Maged Abutaha, (Head of Desert Research Center Herbarium). A fresh sample was designated as voucher specimen CAIH-1255-R has been deposited at the Herbarium of the Desert Research Center in Egypt.

2.3. Extraction and Isolation

The shade dried aerial parts of *K. gijef* (3 kg) were grounded and extracted by 70% aq. MeOH at room temperature to yield *ca.* 106 g of crude extract. The crude extract was suspended in water and partitioned successively with different polarity solvents; *n*-hexane, DCM, EtOAc, and *n*-BuOH respectively. The ethyl acetate extract (8.9 g) was subjected to fractionation using a Biotage Selekt system equipped with a 100 g NP-silica gel, employing gradient elution of *n*-hexane–EtOAc–MeOH; from 1: 0: 0 to 0: 0: 1, yielding six fractions (Fr. A- F). Fr. A (380 mg) was chromatographed using MPLC connected to a prepacked FP ID C18 12 g flash column. It was eluted with H_2O: MeOH: 0.1% FA at a flow rate 30 mL/min, resulting in the isolation of fractions (Fr. A.1.-A.3.). Each of Fr. A.1.-A.3. was further purified using a preparative HPLC column (Inertsil ODS-3, 5 µm, 20 × 250 mm, 10 mL/min) with a gradient of H_2O: MeOH: 0.1% FA, resulting in the isolation of compounds **1, 2, and 3** (10.1 mg, 12.5 mg, and 9.2 mg respectively). Fr. C (1.2 g) was chromatographed *via* MPLC (FP ID C18 24 g, 20 mL/min), and eluted gradually with H_2O: ACN: 0.1% FA (1:0:0.1-0:1:0.1) to yield four subfractions, Fr. C.1.- Fr. C.4. Each subfraction was eluted successively after 20%, 30%, and 35% ACN, respectively. Each subfraction was chromatographed over preparative HPLC, eluted with H_2O: ACN: 0.1% FA (1:0:0.1-0:1:0.1), and further purified using an open column packed with Sephadex LH-20 with 100% MeOH to finally obtain compounds **4, 5**, and **7** (4.9 mg, 5.2 mg, and 3.8 mg, respectively), while compound **6** (5.1 mg) was obtained after further purification over a preparative HPLC column , using an isocratic solvent system of H_2O: ACN: FA 65: 35: 0.1, at a flow rate of 10 mL/ min.

2.4. Spectral Data

*Kedrojiftene A (**4**)*: Amorphous white powder; $[\alpha]_D^{25}$ + 96.8 (*c*, 0.2 MeOH); ^{1}H and APT- NMR data see Table 1 and 2; Negative HRESIMS 713.4122 *m/z* $[M+HCOO]^-$ (calcd. for $C_{37}H_{61}O_{13}$, 713.4112), 703.3818 *m/z* $[M+Cl]^-$ (calcd. for $C_{36}H_{60}O_{11}Cl$, 703.3824).

*Kedrojiftene B (**5**)*: Amorphous white powder; $[\alpha]_D^{25}$ + 14.5 (*c* 0.1, MeOH); ^{1}H and APT- NMR data see Table 1 and 2; Negative HRESIMS *m/z* 715.4286 $[M+HCOO]^-$ (calcd. for $C_{37}H_{63}O_{13}$, 715.4269) *m/z*, 705.3989 $[M+Cl]^-$ (calcd. for $C_{36}H_{62}O_{11}Cl$, 705.3981).

*Kedrojiftene C (**6**)*: Amorphous white powder; $[\alpha]_D^{25}$ + 192.7 (*c* 0.01, MeOH); ^{1}H and APT- NMR data see Table 1 and 2; Negative HRESIMS *m/z* 713.4137 $[M+HCOO]^-$ (calcd. for $C_{37}H_{61}O_{13}$, 713.4112), 703. 3838 *m/z* $[M+Cl]^-$ (calcd. for $C_{36}H_{60}O_{11}Cl$,703.3824).

*Kedrojiftene D (**7**)*: Amorphous white powder; $[\alpha]_D^{25}$ + 39.3 (*c* 0.01, MeOH); ^{1}H and APT- NMR data see Table 1 and 2; Positive HRESIMS $[M+H]^+$ *m/z* 655.4406 (calcd. for $C_{36}H_{63}O_{10}$, 655.4421), $[M+Na]^+$ *m/z* 677.4242 (calcd. for $C_{36}H_{62}O_{10}Na$, 677.4241).

Isolation of new secondary metabolites

2.5. In vitro α-Glucosidase Inhibitory Assay

The in vitro *α*-glucosidase inhibitory activity was assessed following the methodology described by Tao, *et al*., 2013 [10] with some modifications. In brief, samples (5 *μ*L) were dissolved in DMSO and pre-incubated with 45 *μ*L of *α*-glucosidase solution (0.3 U/mL, obtained from SigmaAldrich, Japan) prepared in 50 mM potassium phosphate buffer (pH 7.0). The substrate *p*-nitrophenyl-*α*-D-glucopyranoside (*p*-NPG, purchased from Nacalai Tesque Inc., Kyoto, Japan), was separately prepared in the same buffer system (pH 7.0). The enzymatic reaction was initiated by adding 50 *μ*L of the *p*-NPG substrate solution to the pre-incubated mixture, followed by incubation at 37°C for 10 minutes. After incubation, the reaction was terminated by the addition of 100 *μ*L of 0.5 M Tris-HCl buffer (pH 8.0). The released amount of the *p*-nitrophenol (pNP) was quantified by measuring the absorbance at 405 nm using a 96-well microplate reader (Biotek, Winooski, VT, USA). The percentage of inhibition of *α*-glucosidase activity for each tested sample was calculated according to the following equation:

$$\% \text{ inhibition} = [(\text{average A 405 control} - \text{average A 405 sample})/\text{average A 405 control}] \times 100$$

2.5.1. Statistical Analysis

All samples were assayed in triplicate and expressed as mean ± SD (n = 3) for each value. The t-test was used to determine significant differences. Differences were considered significant if $p < 0.01$ or $p < 0.05$, compared with negative control (DMSO).

3. Results and Discussion

3.1. Structure Elucidation

The phytochemical investigation of the ethyl acetate extract of *K. gijef,* using various chromatographic procedures, led to the isolation of seven compounds (**1-7**). Three phenolics (**1-3**) were identified as 4-hydroxy-3-methoxybenzoic acid **(1)** [11]**,** 4-hydroxybenzoic acid **(2)** [12], and 4-hydroxycinnamic acid **(3)** [12] through analysis of 1D NMR data, HRESIMS, and comparison with the literature.

Compound **4** was isolated as a white amorphous powder. Its molecular formula was deduced to be $C_{36}H_{60}O_{11}$ through negative HRESIMS analysis, displaying peaks at 713.4122 *m/z* $[M+HCOO]^-$ (calcd. for $C_{37}H_{61}O_{13}$, 713.4112) and 703.3818 *m/z* $[M+Cl]^-$ (calcd. for $C_{36}H_{60}O_{11}Cl$,703.3824). This, in conjunction with NMR (^{1}H and APT) spectral data, indicated seven degrees of unsaturation. These findings are consistent with the 36 signals observed in the APT-NMR (Figure S4, S5). Of these, 30 signals were classified based on HSQC (Figure S6, S7) into eight methyls, seven methylenes, and eight methines. The methines included four oxygenated carbons at δ_C 52.6, 69.8, 78.5, and 85.8. Additionally, there were seven quaternary carbons, including three oxygenated carbons at δ_C 65.7, 73.6 and 215.9. The remaining six carbons were assigned to the sugar (hexose) moiety, with a characteristic anomeric carbon (C-1') at δ_C 105.5. The other sugar carbons resonated at δ_C 61.4, 70.4, 74.0, 76.2, and 76.4 (C-2' to C-6'), indicative of the presence of a glucose moiety. The presence of a glucose moiety was further verified by the characteristic downfield shifted signals at δ_H 4.26 (d, J = 7.7 Hz), attributed to the anomeric proton (H-1'). The remaining glucose protons were observed at 3.20-3.85 (H-2' to H-6') in the ^{1}H-NMR spectrum [13, 14] (Figure S3). The aglycone moiety was identified as a tetracyclic triterpene with a cucurbitane nucleus, as indicated by the presence eight methyl signals in NMR spectrum. Five of these signals δ_H 0.75 (s, H_3-18) / δ_C 15.7 (C-18), δ_H 0.91 (s, H_3-28) / δ_C 19.0 (C-28), δ_H 1.16 (s, H_3-19) / δ_C 17.9 (C-19), δ_H 1.19 (s, H_3-30) / δ_C 19.2 (C-30), and δ_H 1.20 (s, H_3-29) / δ_C 24.2 (C-29) were linked to four quaternary carbons (C-13, C-4, C-9, and C-14) within the tetracyclic structure. The locations of the methyl groups were confirmed through analysis of the 2D NMR (HSQC, HMBC, and ^{1}H-^{1}H COSY), as illustrated in Figure 2 and Figures S6-S11).

Four degrees of unsaturation were ascribed to the tetracyclic structure of **4**. One degree was assigned to the carbonyl moiety, another to the sugar moiety, and the remaining degree of unsaturation

was accounted for by an additional cycle. The data suggest that **4** is a polyoxygenated tetracyclic cucurbitane triterpene glycoside with an additional epoxide ring [15].

The trisubstituted epoxide ring was positioned at C-5 (δ_C 65.7) and C-6 δ_H 3.40 (d, J = 5.5 Hz, H-6)/ δ_C 52.6 (C-6), determined by the identified correlations between H-6/ H-7 and H-7/H-8 in the ^{1}H-^{1}H COSY spectrum, alongside with the observed correlations observed between H-3, H_3-28, and H_3-29 with C-5, and H-7 with both C-5 and C-6 in the HMBC spectrum. Also, the carbonyl group was positioned at C-11, evident from the HMBC correlations between H_2-12 and C-11 in the HMBC spectrum, supported by the lack of correlations between H_2-12 and neighboring protons in the^{1}H-^{1}H COSY spectrum, affirming the connection of H_2-12 with two quaternary carbons, specifically C-11 and C-13. The positions of three hydroxyl groups at C-23, C-24, and C-25 were determined based on the correlations observed between H_3-21/H-20, H-20/H-22, H-22/H-23, and H-23/H-24 in the ^{1}H-^{1}H COSY spectrum. This was further supported by, the observed HMBC cross peaks between H_2-22 with C-23 and C-24, and H_3-26 and H_3-27 with C-25 and C-24 in the HMBC spectrum. Additionally, the glucose moiety was linked to C-3, as indicated by the HMBC correlation between H-3/ C-1' and H-1/ C-3 in the HMBC spectrum. The β-orientation of the anomeric carbons in glucose was validated by the significant coupling constant of H-1' δ_H 4.26 (d, J = 7.7 Hz) along with the downfield-shifted signal of C-1 at δ_C 105.5 compared to related metabolites [13, 14]. The NMR spectroscopic data of **4** showed similarities to Bryonioside D, with an additional hydroxyl group at C-23 [15].

The relative spatial arrangement of compound 4 was deduced by analyzing its NOESY spectrum data (Figure 2, Figures S12, S13) and comparing its 1D-NMR data with related metabolites. Specifically, the NOE correlations observed between protons H-3/H-1', H-1'/H-6, and H-6/H_3-28, in conjunction with the absence of correlations between β-oriented H_3-19 with H-6 and H-3, established the α-orientation of H-3 and H-6 as well as the β-orientation of the epoxide ring. Moreover, the absence of correlations between H-23 and H-24 indicated that indicated that these protons are oriented in opposite directions. Furthermore, the correlations observed between well-established β-oriented protons H_3-18/ H-8, H-8/H_3-21, H_3-21/ H-22β, and H-22 β/H-23 indicated that OH-23 was in an α-orientation. Conversely, the correlation observed between H-24 and H-22α suggested that OH-24 was in a β-orientation. Finally, strong consistency between the 1D-NMR analysis of the side chain with related metabolites, alongside the key NOESY correlations, supported the proposal that the deduced structure matched the 23*R* and 24*R* configurations found in cycloccidentalic acid A and Neolasiandroside B [16-18]. Based on the aforementioned observations and analyses, compound **4** was determined to be 5β,6β-epoxy, 23(*R**),24(*R**),25-trihydroxy-3-O-β-D-glucopyranosyl-cucurbita-11-one, and it was identified as kedrojiftene A.

Compound **5** was obtained as a white amorphous powder. The molecular formula $C_{36}H_{62}O_{11}$, was determined through negative HRESIMS, showcasing peaks at *m/z* 715.4286 $[M+HCOO]^-$ (calcd. for $C_{37}H_{63}O_{13}$, 715.4269) and *m/z* 705.3989 $[M+Cl]^-$ (calcd. for $C_{36}H_{62}O_{11}Cl$, 705.3981). The 1D and 2D NMR spectral data corroborated this formula, suggesting a total of six indices of unsaturation.
These results aligned with the 36 signals detected in APT-NMR (Figure S17, S18). Of these, 30 signals were categorized using HSQC (Figure 2 and Figures S17-S20) into eight methyls, seven methylenes, and nine methines. The methines comprised five oxygenated carbons at δ_C 54.2, 67.0, 78.8, 78.8, and 86.7. Furthermore, six quaternary carbons were identified, including two oxygenated carbons at δ_C 68.2 and 73.2. The remaining six carbons were attributed to the sugar (hexose) moiety, with a characteristic anomeric carbon (C-1') at δ_C 105.5. The remaining sugar carbons resonated at δ_C 61.4, 70.4, 74.0, 76.1, and 76.3 (C-2' to C-6'), which were assigned to the glucose moiety.

Compound **5** showed great similarity to compound **4**, differing only in the absence of a carbonyl group and the presence of an additional hydroxyl group at C-11. The correlation observed between H-11, resonating at δ_H 3.76 (J = 11.9, 5.0 Hz), and H-12 δ_H 1.91, (m) and 1.54, (m) in the ^{1}H-^{1}H COSY spectrum (Figure S24), in conjunction with the correlations between H_3-19 and H_2-12 with C-11 in the HMBC spectrum, validates the location of the additional hydroxyl group at C-11 (Figure S22). From the previously mentioned data, we found that compound 5, differing primarily from 5α,6α-Epoxymogroside I E1 in the presence of an additional hydroxyl group at C-23[19].

The relative stereochemistry of **5** was deduced from the analysis of the NOESY spectrum (Figures S25, S26) and by comparing it with data from compounds previously isolated in the literature. The observed correlations between H-11 and the two β-oriented methyls H_3-18 and H_3-19 in

the NOESY spectrum, coupled with the significant coupling constant of H-11 (J = 11.9, 5.0 Hz) [19, 20], indicated that the relative configuration of the OH at C-11 is α- oriented. Additionally, the significant correlations observed between H-1′/H-3, H-3/H-6, and H-6/H_3-28, along with the absence of correlation between H-6, H-3, and H_3-19, implied the α-orientation of H-6 and H-3 as well as the β-orientation of the epoxide ring. Moreover, the correlations observed between H_3-18/ H_3-21, H_3-21/ H-23, H_3-21/H-22β, and H-22β/H-24, coupled with the comparison of the NMR spectra of the side chain of **5** with related metabolites [21-23], suggested that OH-23 and OH-24 were α-oriented, and confirming the proposed structure as 23*R* and 24*S*. From the aforementioned data, **5** was identified as 5β,6β-epoxy-23(*R**),24(*S**),25-trihydroxy-3-O-β-D-glucopyranosyl-cucurbita-11-ol and designated as kedrojiftene B.

Compound **6** was determined to have a molecular formula of $C_{36}H_{60}O_{11}$ based on its negative HRESIMS peaks at *m/z* 713.4137 $[M+HCOO]^-$ (calcd. for $C_{37}H_{61}O_{13}$, 713.4112) and *m/z* 703. 3838 $[M+Cl]^-$ (calcd. for $C_{36}H_{60}O_{11}Cl$, 703.3824). This determination was supported by NMR (^{1}H and APT) spectral data, indicating seven degrees of unsaturation. Compound **6** shared the identical molecular formula with **4**. Upon comparing the ^{1}H and APT data of **6** with those of **4**, we found that compounds **4** and **6** shared the same carbon skeleton of cucurbitane triterpene glycoside.

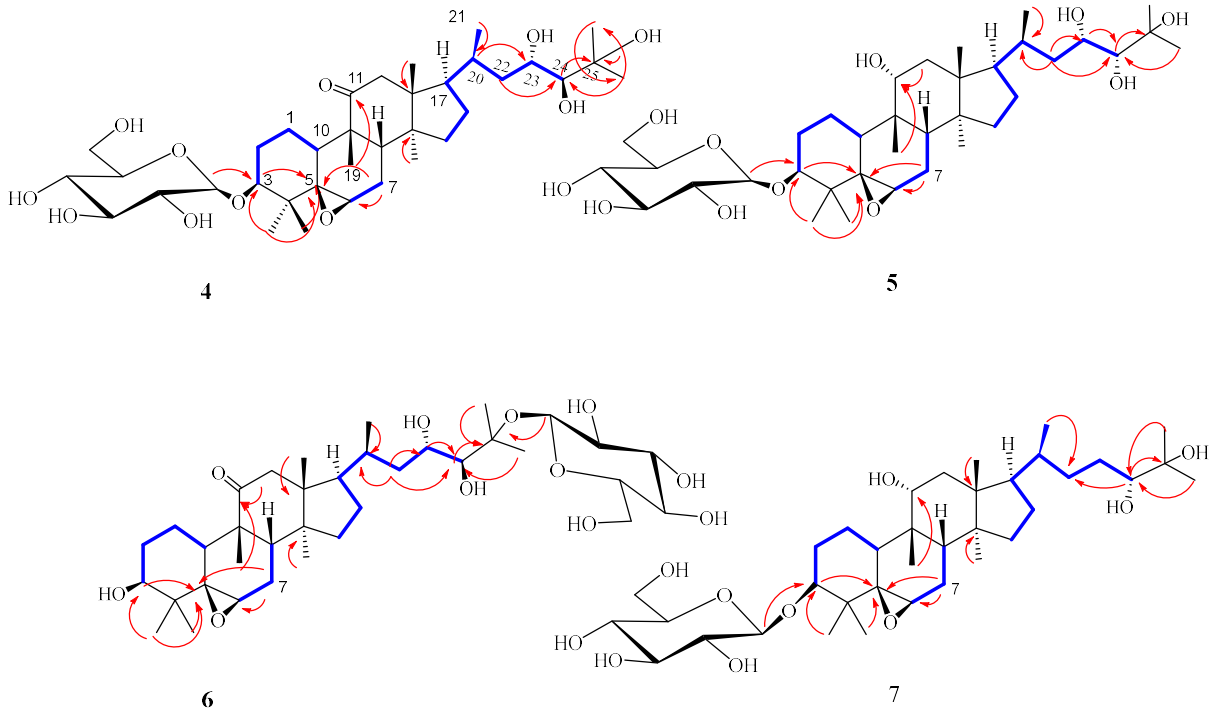

Figure 2: Key HMBC and ^{1}H-^{1}H COSY correlations of compounds **4-7**

By careful examination of the NMR data, we found that they shared the same count of methyls, methines, methylenes, and quaternary carbons, differing primarily in the upfield shift of C-3 (δ_C 76.6) and the downfield shift of C-25 (δ_C 80.4) in **6**, as opposed to the downfield shift of C-3 (δ_C 85.8) and upfield shift of C-25 (δ_C 73.6) in **4**. These shifts in the APT data, accompanied by the identified correlations between H_3-26, H_3-27, and H-1' with C-25, as well as between H-3 with C-2, C-4, C-28, and C-29 in the HMBC spectrum (Figure S34, S35), suggest that the glucose moiety is linked to C-25 in compound **6**, rather than to C-3 as seen in compound **4**. This suggestion is confirmed by the correlations between H-1/H-2 and H-2/H-3 and H-20/H-22, H-22/H-23 and H-23/H-24 in the ^{1}H-^{1}H COSY spectrum (Figure S36, S37).

Table 1. [1]H-NMR Data for Compounds **4-7** (600 MHz, CD_3OD, δ in ppm, J in Hz)

Position	4	5	6	7
1	1.75 (m)	1.82 (m)	1.82 (m)	1.80 (m)
	1.32 (m)	2.38 (m)	1.28 (m)	2.38 (m)
2	1.83 (m)	2.01 (m)	1.73 (m)	1.34 (m)
	2.14 (m)	2.08 (m)	1.88 (m)	2.05 (m)
3	3.48 (br s)	3.47 (br s)	3.46 (br s)	3.47 (br s)
4				
5				
6	3.40 (d, J = 5.5 Hz)	3.36 (m)	3.25 (d, J = 5.5 Hz)	3.36 (m)
7	1.98 (m)	1.85 (m)	1.95 (m)	1.84 (m)
	2.24 (dd, J = 16.7, 9.1 Hz,)	2.18 (m)	2.21 (m)	2.19 (m)
8	1.92 (m)	1.62 (m)	1.89 (m)	1.60 (m)
9				
10	2.41 (dd, J = 12.1, 3.0 Hz)	2.43 (dd, J = 11.7, 2.6 Hz)	2.39 (dd, J = 12.2, 3.1 Hz)	2.42 (dd, J = 11.6, 2.6 Hz)
11		3.76 (dd, J = 11.9, 5.0 Hz)		3.75 (m)
12	3.14 (d, J = 14.4 Hz)	1.91 (m)	3.13 (d, J = 14.5 Hz)	1.86 (m)
	2.45 (d, J = 14.5 Hz)	1.54 (m)	2.44 (d, J = 14.5 Hz)	1.83 (m)
13				
14				
15	1.36 (m)	1.16 (m)	1.43 (m)	1.13 (m)
	1.50 (m)	1.29 (m)	1.31 (m)	1.48 (m)
16	1.47 (m)	1.44 (m)	1.5 (m)	2.01 (m)
	2.08 (m)	2.00 (m)	2.1 (m)	
17	1.78 (m)	1.59 (m)	1.76 (m)	1.61 (m)
18	0.75 (s, 3H)	0.93 (s)	0.74 (s)	0.91 (s)
19	1.16 (s, 3H)	1.23 (s)	1.16 (s)	1.22 (s)
20	1.73 (m)	1.78 (m)	1.75 (m)	1.52 (m)
21	0.97 (d, J = 5.5 Hz)	1.02 (d, J = 6.4 Hz)	0.95 (d, J= 5.6 Hz)	0.99 (d, J = 6.2 Hz)
22	1.47 (m)	0.93 (m)	1.47 (m)	1.28 (m)
	1.55 (m)	1.93 (m)	1.58 (m)	1.53 (m)
23	3.75 (td, J = 8.1, 2.1 Hz)	4.05 (d, J = 10.9 Hz)	3.80 (td, J = 10.7, 1.9 Hz)	1.39 (m), 1.99 (m)
24	3.10 (d, J = 8.3 Hz)	3.05 (br s)	3.38 (d, J = 6.4 Hz)	3.23 (m)
25				
26	1.25 (s)	1.24 (s)	1.36 (s)	1.15 (s)
27	1.24 (s)	1.27 (s)	1.34 (s)	1.18 (s)
28	0.91 (s)	0.88 (s)	0.88 (s)	0.88 (s)
29	1.20 (s)	1.20 (s)	1.15 (s)	1.20 (s)
30	1.19 (s)	0.95 (s)	1.20 (s)	0.95 (s)
1`	4.26 (d, J = 7.7 Hz)	4.26 (d, J = 7.6 Hz)	4.56 (d, J = 7.8 Hz)	4.25 (d, J = 7.5 Hz)
2`	3.31 (m)	3.31 (m)	3.28 (m)	3.31 (m)
3`	3.27 (m)	3.28 (m)	3.17 (m)	3.28 (m)
4`	3.22 (m)	3.23 (m)	3.29 (m)	3.24 (m)
5`	3.36(m)	3.34 (m)	3.38 (m)	3.35 (m)
6`	3.68 (dd, J = 12.0, 5.6 Hz)	3.68 (dd, J = 11.9, 5.6 Hz)	3.85 (dd, J = 11.8, 1.7 Hz)	3.68 (dd, J = 11.7, 5.5 Hz)
	3.85 (dd, J = 11.9, 2.5 Hz)	3.85 (dd, J = 11.9, 2.4 Hz)	3.65 (dd, J = 11.8, 5.4 Hz)	3.85 (dd, J = 11.9, 2.4 Hz)

Table 2. APT- NMR Data for Compounds **4-7** (150 MHz, CD_3OD, δ in ppm)

Position	4	5	6	7
1	19.6	24.2	18.8	24.2
2	28.2	29.6	29.4	29.7
3	85.8	86.7	76.6	87.1
4	40.2	40.5	39.5	40.5
5	65.7	68.2	68.5	68.2
6	52.6	54.2	51.5	54.2
7	22.2	22.5	22.2	22.5
8	42.5	42.0	42.7	42.0
9	48.5	39.1	48.5	39.2
10	33.1	33.8	32.9	33.8
11	215.9	78.8	216.0	78.9
12	48.1	39.5	48.1	39.5
13	48.8	46.0	48.7	45.9
14	48.8	49.3	48.8	49.3
15	34.0	33.9	33.9	33.1
16	27.1	27.3	27.1	27.0
17	50.4	51.3	50.4	50.6
18	15.7	15.8	15.7	15.8
19	17.9	23.6	17.9	23.6
20	31.5	32.0	31.8	35.6
21	17.2	17.7	17.3	17.7
22	40.9	41.8	40.0	33.8
23	69.8	67.0	68.5	27.0
24	78.5	78.8	79.2	78.3
25	73.6	73.2	80.4	72.5
26	22.7	24.6	21.9	23.6
27	26.5	25.9	23.1	24.3
28	19.0	19.7	19.3	19.7
29	24.2	24.7	24.0	24.6
30	19.2	19.8	19.1	19.8
1`	105.5	105.5	96.7	105.6
2`	74.0	74.0	73.9	74.1
3`	76.4	76.3	76.9	76.4
4`	70.4	70.4	70.4	70.4
5`	76.2	76.1	76.5	76.2
6`	61.4	61.4	61.5	61.5

When comparing the structures of 6 with Bryonioside D, a significant difference is noted. This difference is particularly evident in the position of the glucose moiety and the chemical shifts of C-3 and C-23 [15]. The relative stereochemistry of **6** was determined through an analysis of its NOESY spectrum (Figures S38, S39) and by comparing its NMR data with metabolites documented in literature. Specifically, the correlations observed between H_3-28/ H-6, H_3-28/H-3, H_3-19/H-12β, and H-12β/H-11 indicate that the OH at C-11 is α-oriented, while OH-3 is β-oriented. Furthermore, the relative stereochemistry of the side chain was found to be similar to that of **4**, as evidenced by the correlations identified between H_3-18/H-12β, H-12β/ H_3-21, H_3-21/ H-23, and H-24/H-1' alongside the coherent NMR data of compound **6** compared to **4** and related analogues as [24].Thus, compound **6** was characterized as 5β,6β-epoxy-3,23(*R**),24(*R**)-trihydroxy-25-O-β-D-glucopyranosyl-cucurbita-11-one, designated as kedrojiftene C.

Compound **7** was isolated as a white amorphous powder, and the chemical formula was determined to be $C_{36}H_{62}O_{10}$ based on positive HRESIMS $[M+H]^+$ ion peaks at *m/z* 655.4406 (calcd. for $C_{36}H_{63}O_{10}$, 655.4421) and $[M+Na]^+$ *m/z* 677.4242 (calcd. for $C_{36}H_{62}O_{10}Na$, 677.4241). Accordingly, **7** was determined to possess six degrees of unsaturation, and its structure was elucidated through 1D and 2D NMR analyses.

The findings were consistent with the 36 signals detected in the APT-NMR (Figure S43), with 30 of them classified through HSQC (Figures 2 and S45) into eight methyls, eight methylenes, eight methines, including four oxygenated carbons at δ_C 54.2, 78.3, 78.9, and 87.1. Additionally, six quaternary carbons were present, among which were two oxygenated carbons at δ_C 68.2 and 72.5. The remaining six carbons were attributed to the β-glucopyranosyl moiety. Thorough examination revealed that **7** had great structural similarity with **5**, differing solely in possessing three hydroxyl groups instead of four as in **5**. This distinction was notably evident in the side chain, with an upfield shift of C-22 (δ_C 33.8) and C-23 (δ_C 27.0), and a downfield shift of C-22 (δ_C 41.8) and C-23 (δ_C 67) in **7** compared to **5**, respectively. The correlations detected between H-20 and H-22, H-22 and H-23, and H-23 and H-24 in the ^{1}H-^{1}H COSY spectrum (Figures S49, S50) in **7**, paired with the correlations noted between H_3-26, H_3-27 with C-24, C-25, and H_2-22 with C-23 and C-24 in the HMBC spectrum (Figures S47, S48) established the position of hydroxyl groups at C-24 and C-25 similar to 5α,6α -Epoxymogroside I E [19] .

The relative configuration of **7** was determined by comparing its NMR data together with the analysis of NOESY spectrum (Figures S51 and S52). In the NOESY spectrum, correlations such as H-3/ H_3-28, H-3/H-1`, H-3/H-6, and H_3-18/H-11 were observed, while the absence of correlations between H_3-19 with H-3 and H-6 indicated an α-orientation for OH-11 and a β-orientation for the epoxide ring. Additionally, the identical NMR data with previously isolated compounds sharing the same side chain [25-27] suggested an α-orientation for OH-24. This was substantiated by the detected correlations between H-22β/ H-23β and H-23β/ H-24 in the NOESY spectrum. Based on the above data, compound **7** was characterized as 5β,6β-epoxy-24(*R**)-25-diydroxy-3-O-β-D-glucopyranosyl-cucurbita-11β-ol and designated kedrojiftene D.

The biosynthesis of cucurbitane-type triterpenoids, originate from lanosterol, begins with the cyclization of 2,3-oxidosqualene to cucurbitadienol. This initial step is catalyzed by oxidosqualene cyclase (OSC). Subsequent metabolic processes, including hydroxylation, and glucosylation, resulting in diverse array of polyoxygenated and glycosylated cucurbitane triterpenoids. Several enzymes are potentially involved in these various biosynthetic steps, including cytochrome P450 (CYP) and UDP-glucosyltransferase (UGT) [28, 29]

3.2. In vitro α-Glucosidase Inhibitory Assay

Many studies have shown that the phenolic compounds in food and health products can aid in managing control blood sugar [30-32]. α-Glucosidase inhibitors have shown promise not only in diabetes treatment but also in mitigating diet-induced hyperglycemia [32].

The α-glucosidase enzyme is considered as a key glycosidase involved in the metabolic processing of glucose. This enzyme catalyzes the hydrolysis of the α-glucoside bond, consequently releasing simple α-glucose. In our study, we evaluated the inhibitory activity of each compound (**1-7**)

against the α-glucosidase enzyme at a concentration of 500 µg/mL, comparing their effectiveness to DMSO used as the negative control.

The tested compounds exhibited a spectrum of *α*-glucosidase inhibitory activity, spanning from significant or moderate inhibition to weak or negligible effects. The enzyme activity percentages (Figure 3) were 80.5 ± 1.72, 84.9 ± 6.47, and 79.8 ± 1.52, corresponding to inhibition percentages of 19.5%, 15.1%, and 20.2% for compounds (**1**), (**2**), and (**3**), respectively. In contrast, the triterpenoids exhibited weak activity. The reduced activity in (**2**) could be linked to the absence of a methoxy group at C-3, while the slight enhancement in (**5**) might result from substituting the ketone at C-11 with a hydroxyl group.

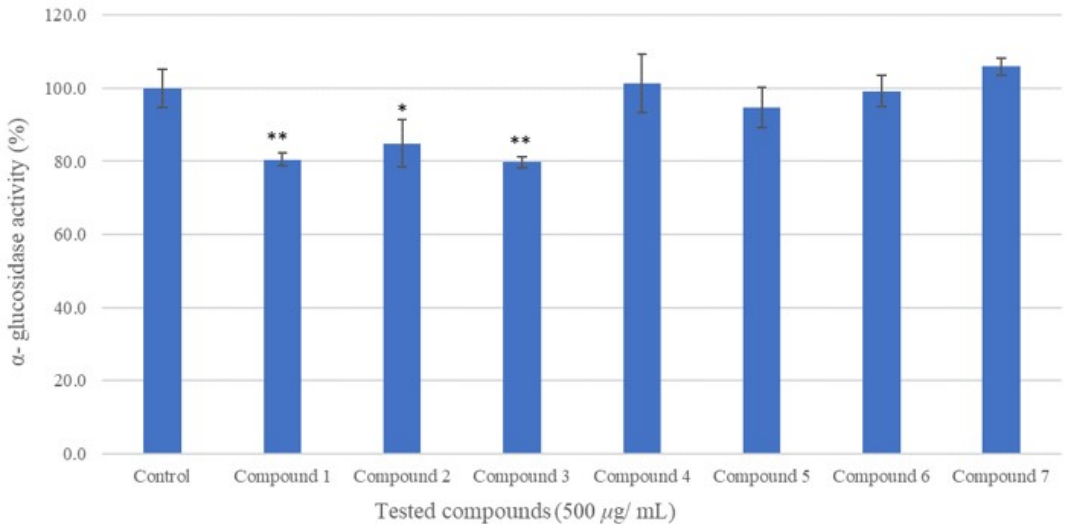

Figure 3. Effect of the isolated compounds (**1-7**) from *K. gijef* on *α*-glucosidase. All compounds were assayed in triplicate and expressed as mean ± SD (n = 3), (**) $p < 0.01$, (*) $p < 0.05$, compared with negative control (DMSO)

Acknowledgments

The first author expresses deep gratitude to Dr. Maged Abutaha, the Head of Desert Research Center Herbarium, for his invaluable assistance in identifying the plant.

Supporting Information

Supporting information accompanies this paper on http://www.acgpubs.org/journal/records-of-natural-products

ORCID

Mahmoud M. Mubarek: 0000-0003-0467-4611
Fahd M. Abdelkarem:0000-0002-6388-0821
Ahmed Othman: 0000-0002-2827-7621
Masako Matsumoto: 0000-0002-8470-0471
Fangjing Li: 0009-0007-0008-8304
Kuniyoshi Shimizu: 0000-0001-5960-1503

References

[1] M. Kousar and J. Park (2023). comparative analysis of the chloroplast genome of *Sicyos angulatus* with other seven species of Cucurbitaceae family, *Genes* **14**, 1776.

[2] K. Pavithra and G. Saravanan (2020). A Review on phytochemistry, pharmacological action, ethanobotanical uses and nutritional potential of *Kedrostis foetidissima* (Jacq.) Cogn, *Cardiovasc. Hematol. Agents Med. Chem.* **18**, 5–20.

[3] P. K. Mukherjee, S. Singha, A. Kar, J. Chanda, S. Banerjee, B. Dasgupta, P. K. Haldar and N. Sharma (2022). Therapeutic importance of Cucurbitaceae: A medicinally important family, *J. Ethnopharmacol.* **282**, 114599.

[4] P. Meenatchi, A. Purushothaman and S. Maneemegalai (2017). Antioxidant, antiglycation and insulinotrophic properties of *Coccinia grandis* (L.) in vitro: Possible role in prevention of diabetic complications, *J. Tradit. Complement. Altern. Med.* **7**, 54–64.

[5] A. Suwannapong, C. Talubmook and W. Promprom (2023). Evaluation of antidiabetic and antioxidant activities of fruit pulp extracts of *Cucurbita moschata* Duchesne and *Cucurbita maxima* Duchesne, *Sci. World J.* **2023**(**1**), 1124606.

[6] K. Pavithra, V. Sathibabu Uddandrao, P. Chandrasekaran, P. Brahmanaidu, S. Sengottuvelu, S. Vadivukkarasi and G. Saravanan (2020). Phenolic fraction extracted from *Kedrostis foetidissima* leaves ameliorated isoproterenol-induced cardiotoxicity in rats through restoration of cardiac antioxidant status, *J. Food Biochem*. **44**(**11**), e13450.

[7] J. O. Unuofin, G. A. Otunola and A. J. Afolayan (2017). Phytochemical screening and in vitro evaluation of antioxidant and antimicrobial activities of *Kedrostis africana* (L.) Cogn, *Asian Pac. J. Trop. Biomed*. **7**, 901-908.

[8] S. Heneidak (2008). Taxonomic revision of wild species of Cucurbitaceae in Egypt, *Taeckholmia* **28**, 21-53.

[9] A. Y. Aldhebiani and N. Mufarah (2017). Phytochemical screening of some wild plants from Wadi Yalmlam, Saudi Arabia, *J. Pharm. Biol. Sci.* **12**, 25-27.

[10] Y. Tao, Y. Zhang, Y. Cheng and Y. Wang (2013). Rapid screening and identification of *α*-glucosidase inhibitors from mulberry leaves using enzyme-immobilized magnetic beads coupled with HPLC/MS and NMR, *Biomed. Chromatogr.* **27**, 148-155.

[11] A. H. Abou Zeid, M. S. Hifnawy and R. S. Mohammed (2009). Phenolic compounds and biological activities of *Dichrostachys cinerea* L, *Med. Aromat. Plant Sci. Biotechnol*. **3**, 42-49.

[12] J.-Y. Cho, J.-H. Moon, K.-Y. Seong and K.-H. Park (1998). Antimicrobial activity of 4-hydroxybenzoic acid and trans 4-hydroxycinnamic acid isolated and identified from rice hull, *Biosci. Biotechnol. Biochem.* **62**, 2273–2276.

[13] X.-S. Li, Q.-L. Wang, Z.-P. Xu, M.-S. Liu, X.-Y. Liang, J.-C. Zheng, H.-Y. Deng, L. Liu, Y.-M. Huang and M.-X. Yang (2024). Structurally diverse cucurbitane-type triterpenoids from the tubers of *Hemsleya chinensis* with cytotoxic activity, *Phytochemistry* **220**, 114033.

[14] N. X. Nhiem, P. V. Kiem, C. V. Minh, N. K. Ban, N. X. Cuong, L. M. Ha, B. H. Tai, T. H. Quang, N. H. Tung and Y. H. Kim (2010). Cucurbitane-type triterpene glycosides from the fruits of *Momordica charantia*, *Magn. Reson. Chem.* **48**, 392–396.

[15] M. Ukiya, T. Akihisa, K. Yasukawa, H. Tokuda, M. Toriumi, K. Koike, Y. Kimura, T. Nikaido, W. Aoi and H. Nishino (2002). Anti-inflammatory and anti-tumor-promoting effects of cucurbitane glycosides from the roots of *Bryonia dioica*, *J. Nat. Prod.* **65**, 179–183.

[16] S.-F. Li, Y.-T. Di, R.-H. Luo, Y.-T. Zheng, Y.-H. Wang, X. Fang, Y. Zhang, L. Li, H.-P. He and S.-L. Li (2012). Cycloartane triterpenoids from *Cassia occidentalis*, *Planta Med.* **78**, 821–827.

[17] L. Lu, J.-C. Chen, H.-J. Song, Y. Li, Y. Nian and M.-H. Qiu (2010). Five new triterpene bisglycosides with acyclic side chains from the rhizomes of *Cimicifuga foetida* L, *Chem. Pharm. Bull.* **58**, 729–733.

[18] Y. Li, N. Hao, S. Ye, Z. Hu, L. Zhao, Y. Qi and X. Tian (2022). New triterpenoid saponins from *Clematis lasiandra* and their mode of action against pea aphids *Acyrthosiphon pisum*, *Ind. Crops Prod.* **187**, 115517.

[19] M. Ukiya, T. Akihisa, H. Tokuda, M. Toriumi, T. Mukainaka, N. Banno, Y. Kimura, J.-i. Hasegawa and H. Nishino (2002). Inhibitory effects of cucurbitane glycosides and other triterpenoids from the fruit of *Momordica grosvenori* on epstein− barr virus early antigen induced by tumor promoter 12-O-tetradecanoylphorbol-13-acetate, *J. Agric. Food Chem.* **50**, 6710–6715.

[20] Y.-J. Wang, J. Yang, X.-N. Li, H. Bai, J.-F. Luo, Z.-R. He and Y.-H. Wang (2022). Cucurbitane-type triterpenoids from the branches and leaves of *Elaeocarpus sylvestris*, *Phytochem. Lett.* **51**, 39–45.

[21] J. Xu, D. Xiao, Q.-H. Lin, J.-F. He, W.-Y. Liu, N. Xie, F. Feng and W. Qu (2016). Cytotoxic tirucallane and apotirucallane triterpenoids from the stems of *Picrasma quassioides*, *J. Nat. Prod.* **79**, 1899–1910.

[22] H. Chen, S. G. Ma, Z. F. Fang, J. Bai, S. S. Yu, X. G. Chen, Q. Hou, S. P. Yuan and X. Chen (2013). Tirucallane triterpenoids from the stems of *Brucea mollis*, *Chem. Biodivers.* **10**, 695–702.

[23] J.-R. Wang, H.-L. Liu, T. Kurtán, A. Mándi, S. Antus, J. Li, H.-Y. Zhang and Y.-W. Guo (2011). Protolimonoids and norlimonoids from the stem bark of *Toona ciliata* var. pubescens, *Org. Biomol. Chem.* **9**, 7685–7696.

[24] M.-J. Tan, J.-M. Ye, N. Turner, C. Hohnen-Behrens, C.-Q. Ke, C.-P. Tang, T. Chen, H.-C. Weiss, E.-R. Gesing and A. Rowland (2008). Antidiabetic activities of triterpenoids isolated from bitter melon associated with activation of the AMPK pathway, *Chem. Biol.* **15**, 263–273.

[25] B. Aslanipour, D. Gülcemal, A. Nalbantsoy, H. Yusufoglu and E. Bedir (2017). Secondary metabolites from *Astragalus karjaginii* BORISS and the evaluation of their effects on cytokine release and hemolysis, *Fitoterapia* **122**, 26-33.

[26] G. Ekiz, S. Duman and E. Bedir (2018). Biotransformation of cyclocanthogenol by the endophytic fungus *Alternaria eureka* 1E1BL1, *Phytochemistry* **151**, 91-98.

[27] T. Savran, D. Gülcemal, M. Masullo, T. Karayildirim, E. Polat, S. Piacente and Ö. Alankus-Çaliskan (2012). Cycloartane glycosides from *Astragalus erinaceus*, *Rec. Nat. Prod.* **6**, 230.

[28] R. Thimmappa, K. Geisler, T. Louveau, P. O'Maille and A. Osbourn (2014). Triterpene biosynthesis in plants, *Annu. Rev. Plant. Biol*. **65**, 225-257.

[29] Y.-C. Kim, D. Choi, A. Cha, Y.-G. Lee, N.-I. Baek, S. Rimal, J. Sang, Y. Lee and S. Lee (2020). Critical enzymes for biosynthesis of cucurbitacin derivatives in watermelon and their biological significance, *Commun. Biol.* **3**, 444.

[30] W. Zhao, Y. Zeng, W. Chang, H. Chen, H. Wang, H. Dai and F. Lv (2023). Potential *α*-glucosidase inhibitors from the deep-sea sediment-derived fungus *Aspergillus insulicola*, *Mar. Drugs* **21**, 157.

[31] D. Semaan, J. Igoli, L. Young, E. Marrero, A. Gray and E. Rowan (2017). In vitro anti-diabetic activity of flavonoids and pheophytins from *Allophylus cominia* Sw. on PTP1B, DPPIV, alpha-glucosidase and alpha-amylase enzymes, *J. Ethnopharmacol.* **203**, 39-46.

[32] T. J. Ha, S. B. Song, J. Ko, C.-H. Park, J.-M. Ko, M.-E. Choe, D.-Y. Kwak and J. H. Lee (2018). Isolation and identification of α-glucosidase inhibitory constituents from the seeds of *Vigna nakashimae*: Enzyme kinetic study with active phytochemical, *Food Chem*. **266**, 483-489.